



Short communication

Non-porous activated mesophase carbon microbeads as a negative electrode material for asymmetric electrochemical capacitors

Cheng Zheng^{a,b}, Jichao Gao^{a,b}, Masaki Yoshio^c, Li Qi^a, Hongyu Wang^{a,*}

^a State Key Laboratory of Electroanalytical Chemistry, Changchun Institute of Applied Chemistry, Chinese Academy of Sciences, 5625 Renmin Street, Changchun 130022, China

^b Graduate University of Chinese Academy of Sciences, Beijing 100039, China

^c Advanced Research Center, Saga University, 1341 Yuga-machi, Saga 840-0047, Japan

HIGHLIGHTS

- Non-porous activated MCMB as a negative electrode in electrochemical capacitors.
- It elevates both energy and power densities.
- The initial cation intercalation into MCMB causes irreversible structure change.
- Spiro-(1,1')-bipyrrolidinium enlarges the storage capability of MCMB remarkably.

ARTICLE INFO

Article history:

Received 11 October 2012

Received in revised form

7 December 2012

Accepted 8 December 2012

Available online 27 December 2012

Keywords:

Mesophase carbon microbeads

Electrochemical capacitors

Quaternary alkyl ammonium

Activated carbon

Spiro-(1,1')-bipyrrolidinium

ABSTRACT

Non-porous activated (mesophase carbon microbeads) MCMBs have been prepared by calcinations at 1100 °C and then activated with KOH at 800 °C in a nitrogen flow. This spherical carbon material could store a large number of ions after having been subjected to an “extra” electrochemical activation. It has been used as the negative electrode for asymmetric electrochemical capacitors of MCMB/activated carbon. The charge storage mechanism at the MCMB negative electrode has been investigated by XRD and TEM. The results demonstrate that the intercalation of quaternary alkyl ammonium cations from the electrolytes causes an irreversible expansion of interlayer spaces between adjacent carbon layers, which provides accommodation for subsequent ion adsorption. A series of quaternary alkyl ammonium-based electrolytes have been tested in the capacitors and the effect of the cation has been studied. Spiro-(1,1')-bipyrrolidinium increases the storage ability most significantly although it is not the lightest quaternary alkyl ammonium cation.

© 2013 Elsevier B.V. All rights reserved.

1. Introduction

Nowadays, electric double layer capacitors (EDLCs) with two symmetrical activated carbon (AC) electrodes prevail in the world. To meet the urgent needs of elevated energy density, more and more research effort has been devoted to asymmetric hybrid capacitors consisting of battery-type electrode materials and organic electrolytes [1–5]. In the history of electric storage devices, carbon has stood out from numerous electrode materials by virtue of multiple advantages. And so does in electrochemical capacitors today. There have emerged some types of asymmetric capacitors using both carbon-related electrodes. For instance, the AC/graphite capacitors exceed common EDLCs in energy density [6–13]. In contrast, lithium-ion capacitors comprising Li-doped carbon negative and AC positive

electrodes in Li⁺-electrolytes possess significantly enlarged energy densities [14]. However, the hazard risk of Li metal deposition at the surface of the negative electrode can't be completely excluded. From this viewpoint, graphite/AC capacitors using quaternary alkyl ammonium-based organic electrolytes are privileged [15].

Another big improvement in carbon-based capacitors was the work on “Nanogate Carbon®” [16,17]. This type of carbon electrode demonstrates astonishing ability to accommodate ions in spite of the limited specific surface area. Here we also call it as non-porous activated soft carbon (NPASC). The storage mechanism of ions at a NPASC electrode involves the intercalation of ions into the interlayer space between adjacent graphene layers [18,19]. Although a capacitor composed of two symmetrical NPASC electrodes has high energy density, it experiences drastic stress due to the big volume change of both NPASC electrodes during charge–discharge processes [19], which is a problem in practical applications. Therefore, we propose a kind of asymmetric capacitors composed of

* Corresponding author. Tel./fax: +86 431 85262287.

E-mail addresses: hongyuwang@ciac.jl.cn, wanghongyu@hotmail.com (H. Wang).

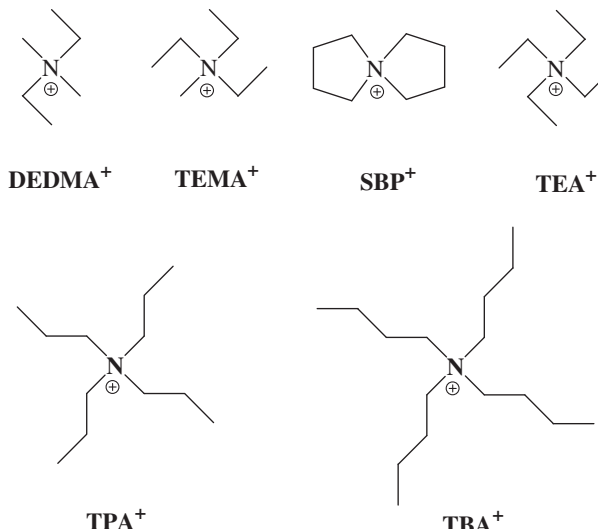


Fig. 1. Chemical structures of quaternary alkyl ammonium cations.

NPASC and AC electrodes in quaternary alkyl ammonium-based organic electrolytes in this study. The volume change at the AC electrode is negligible, so the stress within a capacitor can be considerably lessened. On the other hand, to mitigate the adverse mechanical effects at the NPASC electrode, the spherical shape of particles is advantageous. Because spheres can slide and rotate freely with each other, and then considerably disturbs the preferential orientation of graphene layers as in the “anisotropic” electrode composed of plate- or needle-like particles. Then the volume change of a spherical NPASC particle can be isotropically dispersed into different directions during the course of adsorption and desorption of ions. Consequently, MCMBs (mesophase carbon microbeads) were employed [20] as the precursor of spherical NPASC in this work. The merits are apparent. First, its small surface area is typical of non-porous feature. Second, its relatively high packing density increases volumetric energy density of capacitor. Third, the outer surface of MCMB is mainly composed of edge plane, which is much more chemically sensitive than basal plane of graphene layers. So the activations become quite efficient. Fourth, MCMB has been applied in industry for several decades. Here we will show that non-porous activated MCMB is a promising negative electrode material for asymmetric capacitors. Moreover, the effect of quaternary alkyl ammonium cation on the electrochemical performance of this electrode material has also been addressed.

2. Experimental

2.1. Preparation of non-porous activated MCMB

Crude MCMB was prepared from coal tar pitch by Beiterui Co. Ltd. The as-received MCMB was heated in a nitrogen flow at 1100 °C for 6 h to fulfill the carbonization. Then the carbonized MCMB is mixed

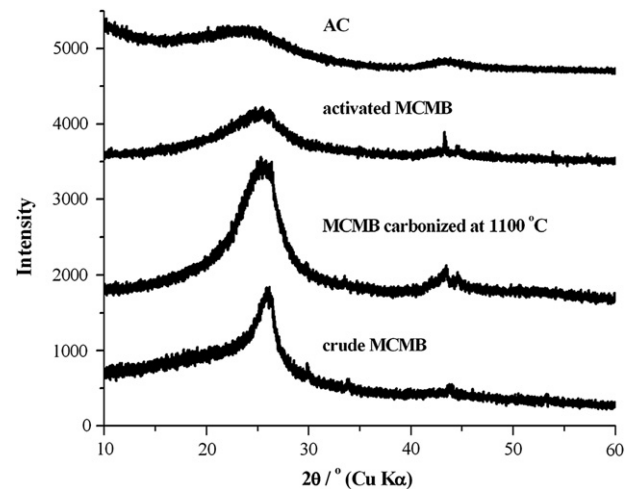


Fig. 3. XRD patterns of the carbon materials.

with KOH at the weight ratio of 1 to 4 and heated in a nitrogen flow at the temperature of 800 °C for 2 h. This KOH-activated MCMB was rinsed with distilled water to get rid of most of KOH and dried.

2.2. Electrochemical measurements

The AC was PW15M13130 from Kureha Co. Ltd. and its physical properties have been described in the past reports [12,13]. In a capacitor (coin cell), the weight ratio of negative to positive electrode materials was kept at 1. The electrolytes were 1 M quaternary alkyl ammonium salts dissolved in propylene carbonate (PC) solvent. BF_4^- was the counter anion in these salts. The quaternary alkyl ammonium cations consisted of diethyldimethyl ammonium (DEDMA⁺), trimethylmethyl ammonium (TEMA⁺), tetraethyl ammonium (TEA⁺), tetrapropyl ammonium (TPA⁺), tetrabutyl ammonium (TBA⁺) and spiro-(1,1')-bipyrrolidinium (SBP⁺), as shown in Fig. 1. The coin cell fabrication and glove box conditions were similar to those described in the past reports [12,13]. The galvanostatic charge–discharge tests of the coin cells were generally performed at the constant current density of 0.4 mA cm⁻². Unless otherwise specified, the cut-off voltages were 0 and 2.7 V for the EDLCs with two symmetrical AC electrodes. In the case of asymmetric capacitors, the cut-off voltages were set at 0 and 3.5 V. Charge storage ability of the total capacitor (coin cell) was expressed in the terms of capacity (mAh g⁻¹). The capacity values were calculated according to the following formula: $Q = IT/w_+$ (I , the constant current (mA); T , the time for charge or discharge between cut-off voltages (h); w_+ , the weight of the positive electrode material (g)).

3. Results and discussion

Fig. 2 compares the SEM images of the MCMB samples in this study. After the carbonization treatment, the MCMB sample (BET

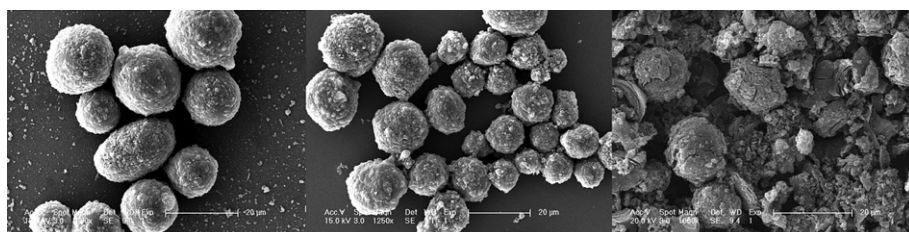


Fig. 2. SEM images of MCMB samples: original MCMB, MCMB carbonized at 1100 °C, and activated MCMB (from left to right).

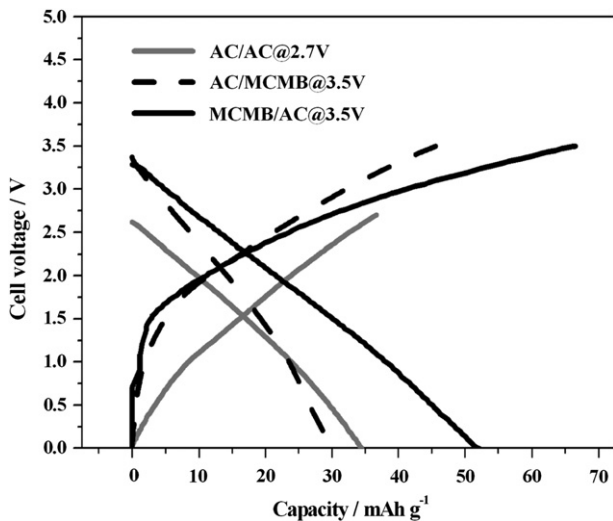


Fig. 4. Initial galvanostatic charge–discharge curves of symmetrical and asymmetric capacitors using the electrolyte of 1 M TEABF₄ dissolved in PC.

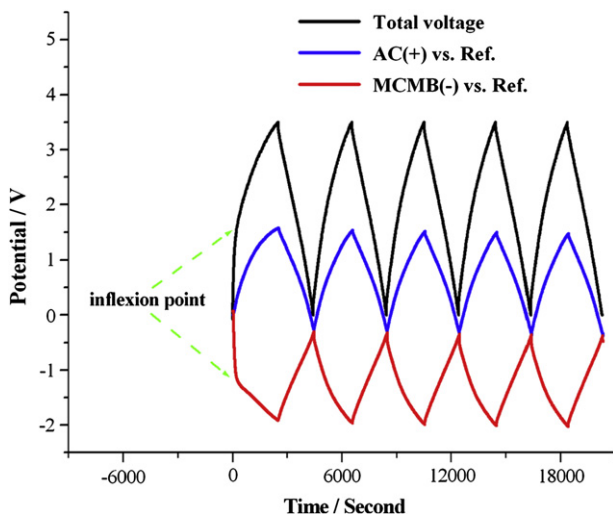


Fig. 5. Potential profiles of electrodes versus a heavy AC reference electrode in an MCMB/AC capacitor during galvanostatic charge–discharge. Electrolyte: 1 M TEABF₄ dissolved in PC.

specific surface area, 0.53 m² g⁻¹) has tiny change on the external surface. In contrast, the activated MCMB sample maintains the spherical shape after the carbonization and activation treatments, while the surface becomes rough (BET specific surface area, 34.06 m² g⁻¹). The tap density of this MCMB sample is 0.662 g cm⁻³, bigger than that of the AC sample (0.494 g cm⁻³) in this study. From their XRD patterns (Fig. 3), these MCMB samples belong to soft carbon.

Fig. 4 compares the initial galvanostatic charge–discharge curves of the symmetrical and asymmetric capacitors. Both the asymmetric capacitors are superior to the symmetrical AC/AC capacitor in the terms of high working voltage (3.5 V). Traditional EDLCs composed of two AC electrodes can't tolerate high voltage over 2.7 V, otherwise the burst of the capacitor occurs because the high surface area of AC electrode is liable to electrolyte decomposition. In contrast, a non-porous carbon electrode with small surface area can extend the electrochemical window to a wider range. Furthermore, the MCMB/AC capacitor delivers a much higher capacity value than the other asymmetric capacitor (AC/MCMB). This fact implies that MCMB may be a suitable negative electrode material rather than a positive one in an asymmetric capacitor. In addition, a bent-line feature can be observed in the initial charge curve of the asymmetric capacitors. By introducing a heavy AC reference electrode into a capacitor [7,11], we could synchronously monitor the respective potential changes of either the positive or negative electrodes during the galvanostatic charge–discharge cycles as depicted in Fig. 5. In an MCMB/AC capacitor, the potential profile of AC positive electrode consists of simply straight lines characteristic of EDLC. In contrast, the potential profile of the MCMB negative electrode has an anomalous behavior in the 1st-cycle charge process. It drops down abruptly just after the galvanostatic charge of the total capacitor starts. This trend is correlative with the limited surface area of the MCMB electrode, which can scarcely store cations through EDLC mechanism. At a certain inflection point, the descending pace of the potential curve slows down, and then a sloping line spreads out. This sloping section was ascribed to the intercalation of cations into the interlayer spaces between adjacent graphene layers of NPASC [21]. In the subsequent procedures, all the potential profiles of MCMB are completely tuned to linear sloping curves, which obey the EDLC mode.

The electrochemical activation upon NPASC is principally fulfilled by the intercalation of ions in the initial charge process [16–20]. Reversible intercalation/de-intercalation of some ions into/from graphite electrode is common. However, this electrochemical

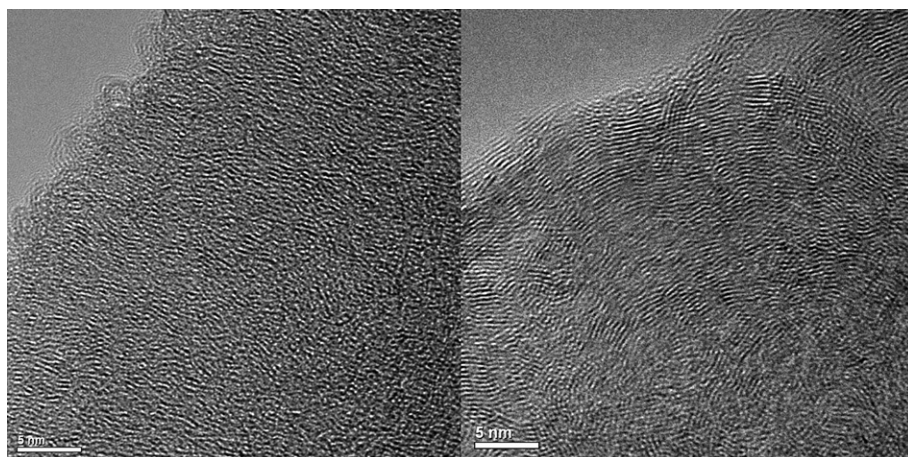


Fig. 6. HRTEM images of MCMB negative electrode before (left) and after (right) the initial galvanostatic charge–discharge in an asymmetric capacitor using the electrolyte of 1 M TEABF₄ dissolved in PC.

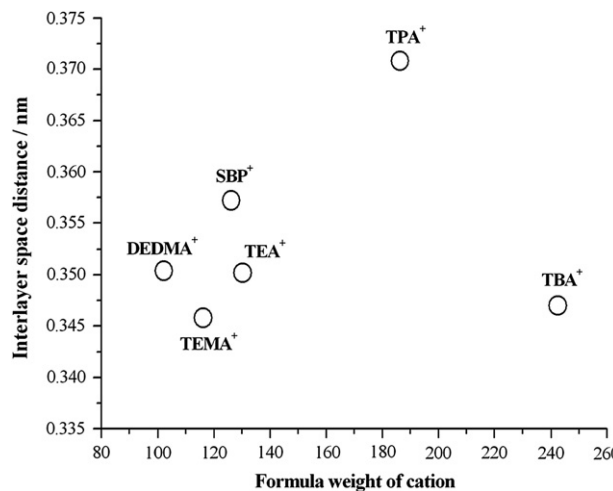


Fig. 7. The interlayer space distance values of MCMB after 1st-cycle charge–discharge of MCMB/AC capacitors using different electrolytes versus the formula weight of cation in the electrolyte.

activation of NPASC is an irreversible process. As shown in Fig. 6, an MCMB negative electrode demonstrates contrastive high resolution transmission electron microscope (HRTEM) images before and after the initial galvanostatic charge–discharge cycle. In the original electrode material, small carbon layers are arranged chaotically, and the interstitials are too narrow to be precisely measured. In contrast, after the 1st-cycle galvanostatic charge–discharge of the capacitor, the local alignment of carbon layers in MCMB gets somehow ordered and the interlayer spaces become broader, which don't return to the original state although most of the cations have been removed from the electrode in the discharge state. TEM images of MCMB electrochemically activated by various cations provided respective interlayer space distance values, as compared in Fig. 7. There is no clear relationship between the cation size (formula weight) and the interlayer space distance. Actually, the expansion extent of the interlayer space may depend on not only the cation size, but also other factors such as the amount of cations intercalated. So neither the biggest nor the smallest cation, but TPA⁺ results in the top interlayer space distance value of MCMB. From the viewpoint of volume change, TPA⁺-based electrolytes are not a good choice for a MCMB/AC capacitor. XRD studies on similarly treated MCMB (Fig. 8)

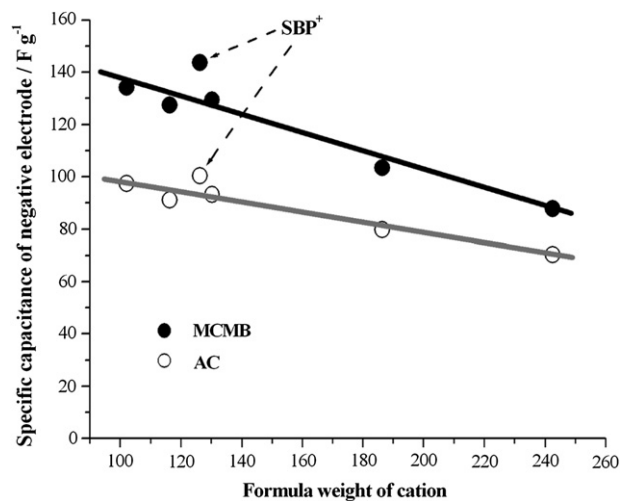


Fig. 9. Relationship between the specific capacitance of negative electrodes (MCMB and AC) and the formula weight of cation.

agree with the TEM results. They reveal the shift of (002) peak to lower diffraction angles, indicating the expansion of interlayer spaces. However, the effect of cation on the extent of (002) peak shift is not discernible.

In fact, from the potential profile of an electrode during the initial discharge process (Fig. 5), we could calculate its specific capacitance value [7,11]. Therefore, the storage ability of negative electrodes toward different cations can be clearly evaluated as illustrated in Fig. 9. For each cation, MCMB surpasses AC as a negative electrode. Moreover, for both MCMB and AC electrodes, the specific capacitance value almost decreases linearly with the increase of formula weight of cation, and MCMB appears more sensitive than AC. Astonishingly, the SBP⁺ gives rise to the extraordinary storage ability although it is not the lightest cation. This phenomenon may be linked with its “small size and rigidity” [22]. So SBP⁺-based organic electrolytes are quite suitable for these capacitors.

On the other hand, the formula weight of cation may also influence the power density of capacitors. As shown in Fig. 10, for both types of capacitors, the power density value declines with the increase of formula weight of cation. This fact can be easily envisaged since the more heavy a cation is, the more sluggish it moves in

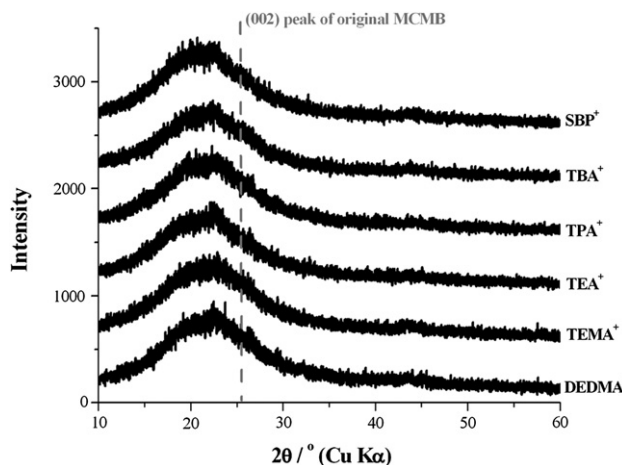


Fig. 8. XRD patterns of MCMB negative electrode after the initial galvanostatic charge–discharge of MCMB/AC capacitors containing different cations.

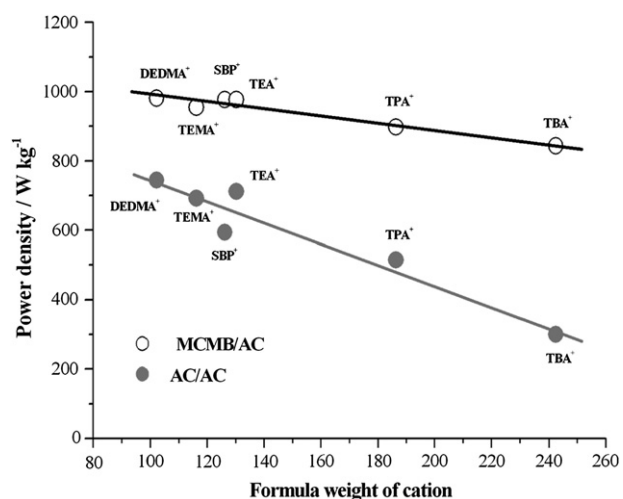


Fig. 10. Relationship between the power density of the MCMB/AC and AC/AC capacitors under the current density of 1.2 A g^{-1} and the formula weight of cation.

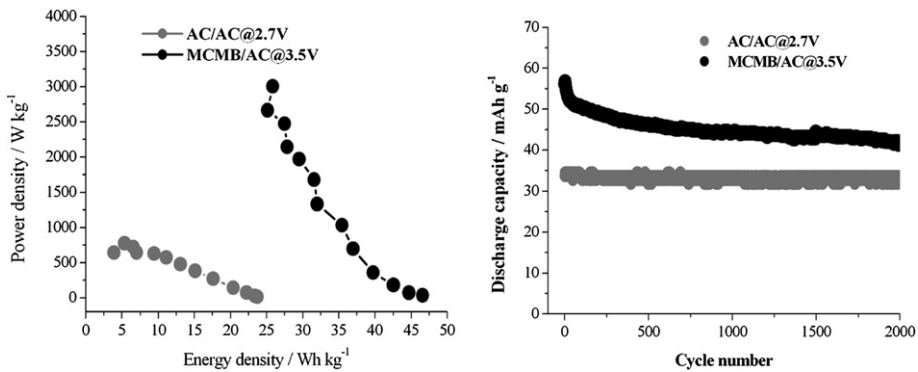


Fig. 11. Ragone plots (left) and cycle life test (right) of the AC/AC and MCMB/AC capacitors using the electrolyte of 1 M SBPBF₄ dissolved in PC.

both the phases of electrode matrix and electrolyte solutions. It is intriguing to note here that the power density of an asymmetric capacitor appears more inert than that of an EDLC in response to the change of formula weight of cation. This merit of the asymmetric capacitors may be ascribed to the “*in situ*” adjusted channel for cation transportation in MCMB by the initial intercalation of cations.

Fig. 11 compares the performance of a traditional EDLC and the MCMB/AC capacitor using the electrolyte of 1 M SBPBF₄ dissolved in PC. From the Ragone plots, the asymmetric capacitor possesses both higher energy and power densities than the EDLC. As for the cycleability, the asymmetric capacitor demonstrates a descending trend in the storage ability. However, the capacity of the asymmetric capacitor is still larger than the EDLC after certain long cycles. Further work in improving its cycle life is carried out. There are some promising methods may be effective in coping with this problem, such as the surface treatment of MCMB electrode material or some modifications of the electrolyte solutions.

4. Conclusion

We have shown that a non-porous activated MCMB material is a satisfactory negative electrode in the asymmetric capacitor using quaternary alkyl ammonium-based organic electrolytes. In addition, the SBP⁺ cation helps increase the storage ability of the negative electrode remarkably. The power density values of the asymmetric capacitor decreases as the formula weight of cation become big. However, this trend is less apparent than that of common EDLCs.

Acknowledgments

This work was financially supported by National Natural Science Foundation of China (21173206), National Basic Research Program

of China (2011CB935702), Scientific Research Foundation for the Returned Overseas Chinese Scholars and State Education Ministry (SRF for ROCS, SEM) and Hundred Talents Program of Chinese Academy of Sciences.

References

- [1] G.G. Amatucci, F. Badway, A. DuPasquier, T. Zheng, J. Electrochem. Soc. 148 (2001) A930–A939.
- [2] K. Naoi, S. Suematsu, M. Hanada, H. Takenouchi, J. Electrochem. Soc. 149 (2002) A472–A477.
- [3] D. Villers, D. Jobin, C. Soucy, D. Cossement, R. Chahine, L. Breau, D. Bélanger, J. Electrochem. Soc. 150 (2003) A747–A752.
- [4] A. Laforgue, P. Simon, J.F. Fauvarque, M. Mastragostino, F. Soavi, J.F. Sarrau, P. Lailler, M. Conte, E. Rossi, S. Saguatti, J. Electrochem. Soc. 150 (2003) A645–A651.
- [5] H. Li, L. Cheng, Y.Y. Xia, Electrochim. Solid-State Lett. 8 (2005) A433–A436.
- [6] H. Wang, M. Yoshio, Electrochim. Commun. 8 (2006) 1481–1486.
- [7] H. Wang, M. Yoshio, A.K. Thapa, H. Nakamura, J. Power Sources 169 (2007) 375–380.
- [8] H. Wang, M. Yoshio, Electrochim. Commun. 10 (2008) 382–386.
- [9] H. Wang, M. Yoshio, J. Power Sources 177 (2008) 681–684.
- [10] H. Wang, M. Yoshio, J. Power Sources 195 (2010) 389–392.
- [11] H. Wang, M. Yoshio, J. Power Sources 195 (2010) 1263–1265.
- [12] H. Wang, M. Yoshio, Chem. Commun. 46 (2010) 1544–1546.
- [13] Y. Wang, C. Zheng, L. Qi, M. Yoshio, K. Yoshizuka, H. Wang, J. Power Sources 196 (2011) 10507–10510.
- [14] V. Khomenko, E. Raymundo-Piñero, F. Béguin, J. Power Sources 177 (2008) 643–651.
- [15] H. Wang, M. Yoshio, J. Power Sources 200 (2012) 108–112.
- [16] M. Takeuchi, K. Koike, T. Maruyama, A. Mogami, M. Okamura, Electrochemistry 66 (1998) 1311–1317.
- [17] M. Takeuchi, T. Maruyama, K. Koike, A. Mogami, M. Okamura, Electrochemistry 69 (2001) 487–492.
- [18] P.W. Ruch, M. Hahn, D. Cericola, A. Menzel, R. Kötz, A. Wokaun, Carbon 48 (2010) 1880–1888.
- [19] T. Ohta, I. Kim, M. Egashira, N. Yoshimoto, M. Morita, J. Power Sources 198 (2012) 408–415.
- [20] M. Yoshio, R.J. Brodd, A. Kozawa (Eds.), Lithium-Ion Batteries, Springer Science + Business Media, LLC, 2009, p. 66.
- [21] H. Yoo, Y. Park, J. Ryu, S. Oh, Electrochim. Acta 56 (2011) 9931–9936.
- [22] K. Chiba, T. Ueda, H. Yamamoto, Electrochemistry 75 (2007) 664–667.